Astron. Astrophys. 334, 221–238 (1998)

ASTRONOMY AND ASTROPHYSICS

Spectroscopic analyses of the parent stars of extrasolar planetary system candidates

Guillermo Gonzalez

Astronomy Department, University of Washington, Box 351580, Seattle, WA 98195-1580, USA (gonzalez@astro.washington.edu)

Received 9 September 1997 / Accepted 9 February 1998

Abstract. The stars ρ^1 Cnc, ρ CrB, 16 Cyg B, 51 Peg, 47 UMa, 70 Vir, and HD 114762 have recently been proposed to harbor planetary mass companions based on small amplitude radial velocity variations. From spectroscopic analyses we derive the following values of [Fe/H] for these stars: 0.29, -0.29, 0.06, 0.21, 0.01, -0.03, and -0.60 (all with an uncertainty of 0.06 dex), respectively; the [Fe/H] value for 16 Cyg A is 0.11. The four 51 Peg-like systems, υ And, τ Boo, ρ^1 Cnc, and 51 Peg, have a mean [Fe/H] value of 0.25. Otherwise, the abundance patterns, expressed as [X/Fe], are approximately solar.

We used Fourier analysis, supplemented by line profile synthesis, to derive the following $v \sin i$ values: < 1.3, 1.4 ± 0.3, 1.7 ± 0.4, < 0.5, and < 1.5 km s^{-1} for ρ^1 Cnc, 51 Peg, 47 UMa, 70 Vir, and HD 114762, respectively. A similar analysis of the spectrum of ρ CrB (with a lower resolving power) yields a value of $\sim$1.5 km s^{-1}. Combining these data with published estimates of $v \sin i$ and rotation periods and assuming that the radial velocity variations are due to the presence of planets, we derive the following masses for the companions: > 0.66, $2.9^{+13.6}_{-1.3}$, 0.49 ± 0.03, $3.4^{+3.1}_{-1.1}$, > 9.4, and $> 10.4\ \mathcal{M}_{\rm J}$ for ρ^1 Cnc, ρ CrB, 51 Peg, 47 UMa, 70 Vir, and HD 114762, respectively; the mass of 16 Cyg B b, calculated using a published estimate for $\sin i$, is $2.0^{+1.1}_{-0.3}\ \mathcal{M}_{\rm J}$. The masses of the companions to υ And and τ Boo, which were analyzed in a previous paper, are $0.76^{+0.19}_{-0.03}$ and $5.9^{+43.9}_{-1.8}\ \mathcal{M}_{\rm J}$, respectively.

We confirm previous claims that ρ^1 Cnc appears to be a subgiant. However, the theoretical isochrone-derived age is much greater than the age of the universe. At this time we have insufficient data to determine the true nature of ρ^1 Cnc, but we suggest that it may be an unresolved stellar binary viewed nearly pole-on. A search for line profile variations might help to resolve this mystery.

Our findings are consistent with a recently proposed mechanism whereby a gas giant migrates to within a few hundredths of an AU of its parent star during the formative epoch of the planetary system, and the material between the planet and the star is accreted onto the latter. If the accreted material is depleted in H and He, then the photospheric composition of the parent star might be altered significantly.

Key words: stars: abundances – planetary systems

1. Introduction

Between October 1995 and July 1997 eight candidate extrasolar planetary systems were announced by groups searching for radial velocity variations among solar-type stars: 51 Peg (Mayor & Queloz 1995 and Marcy et al. 1997); 47 UMa (Butler & Marcy 1996); 70 Vir (Marcy & Butler 1996); ρ^1 Cnc, τ Boo, υ And, (Butler et al. 1997); 16 Cyg B (Cochran et al. 1997); ρ CrB (Noyes et al. 1997). To these we can add HD 114762 (Latham et al. 1989). These historic discoveries are the fruits of about 15 years of searching by several groups (Campbell et al. 1988; Cochran & Hatzes 1994; Walker et al. 1995), which had not, until now, found evidence of planetary mass companions. With these finds, we finally have empirical data to test planet formation models. One aspect of planet formation that has not been discussed in much detail is the dependence of planet formation on the metallicity of the protostellar cloud. With nine planetary-system candidates (and one certain case, the Solar System), we can begin to address this question.

The primary purpose of this study is to determine accurately the metallicities of the photospheres of ρ^1 Cnc, ρ CrB, 16 Cyg A and B, 51 Peg, 47 UMa, 70 Vir, and HD 114762 (the stars υ And and τ Boo have been analyzed by Gonzalez 1997; Paper I); in addition, we determine the abundances of about 15 other elements including lithium. Also, we compare the abundance patterns of 16 Cyg B with its companion, 16 Cyg A, which does not display regular radial velocity variations (Cochran et al. 1997). While others have performed separate abundance analyses on all these stars already, we have analyzed them together as a homogenous group for the first time, therefore minimizing the relative systematic errors, and, unlike most previous studies, we make use of high-quality spectra. In addition, we employ modern model atmospheres. As a secondary goal, we also derive estimates of $v \sin i$ for these stars (except 16 Cyg A and B), and, combining them with other data, employ them to place constraints on the masses of the companions (assuming the radial velocity variations are not intrinsic to the stars). We end with a discussion of the metallicity trends among the parent stars of the extrasolar planets.

Table 1. Atomic data for lines used in the analysis of the Group 1 stars and not listed by Gonzalez & Lambert (1996)

Species	λ(Å)	χ_1 (eV)	$W_\lambda(m\text{Å})_\odot$	$\log gf$
C I	6587.61	8.53	13.0	−1.20
O I	7771.94	9.14	70.6	0.25
O I	7774.16	9.14	62.7	0.13
O I	7775.38	9.14	48.4	−0.11
Na I	5688.20	2.10	121.4	−0.65
Al I	7835.29	4.02	45.0	−0.74
Al I	7836.11	4.02	58.6	−0.57
Si I	5793.06	4.93	44.3	−1.96
Ca I	5867.55	2.93	24.7	−1.62
Ca I	6455.59	2.52	57.3	−1.40
Cr I	5783.07	3.32	32.5	−0.45
Cr I	5783.87	3.32	44.7	−0.21
Fe I	6089.57	5.02	37.0	−0.91
Fe I	6093.65	4.61	31.0	−1.40
Fe I	6498.94	0.96	46.3	−4.69
Fe I	6574.25	0.99	28.3	−5.04
Fe I	6581.22	1.48	19.0	−4.79
Fe I	6591.33	4.59	10.7	−2.04
Fe I	6710.30	1.48	16.0	−4.89
Fe I	6739.51	1.56	11.7	−4.97
Fe I	7583.78	3.02	85.7	−1.95
Fe I	7586.01	4.31	135.3	−0.20
Fe I	7588.29	5.03	28.0	−1.14
Co I	6454.98	3.63	14.5	−0.32

Table 2. Atomic data for lines used in the analysis of ρ CrB and not listed in Paper I

Species	λ(Å)	χ_1 (eV)	$W_\lambda(m\text{Å})_\odot$	$\log gf$
C I	5380.31	7.68	20.5	−1.71
C I	6587.61	8.53	16.5	−1.08
O I	7771.94	9.14	66.6	0.19
O I	7774.16	9.14	61.8	0.11
O I	7775.38	9.14	48.6	−0.11
Si I	6721.85	5.86	45.3	−1.14
Sc II	5526.80	1.77	74.9	0.10
Ti I	6261.09	1.43	51.6	−0.46
Ti II	5336.78	1.58	71.7	−1.61
Ti II	5418.77	1.58	51.0	−2.07
Fe I	5322.04	2.28	62.6	−2.86
Fe I	6024.69	4.55	112.1	−0.12
Fe I	6213.43	2.22	83.2	−2.58
Fe I	6265.14	2.18	85.6	−2.57
Fe I	6710.30	1.48	16.8	−4.80
Fe I	6733.15	4.64	26.2	−1.45
Fe I	6739.52	1.56	12.0	−4.90
Fe II	5234.62	3.22	85.4	−2.20
Fe II	6247.56	3.89	54.1	−2.30

2. Observations

Spectra of moderate resolving power ($R \approx 60,000$) of the Group 1 stars[1] were obtained by the author on six observing runs of two to three nights each between December 1995 and November 1996 at McDonald Observatory using the 2.1 m telescope equipped with the Sandiford Cassegrain echelle spectrograph (McCarthy et al. 1993) and a 1200 x 400 pixel Reticon CCD. Each star was observed at most once per night with exposure times typically between one and five minutes, resulting in spectra with S/N ratios between 150 and 300. In addition, a spectrum of ρ CrB was obtained by David Lambert at the request of the author in June 1997, with the McDonald Observatory 2.7 m telescope equipped with an echelle spectrograph at the coudé focus (Tull et al. 1995). The 2048x2048 Tektronix CCD resulted in a resolving power of 65,000 and a S/N ratio of 300. The stars studied in Paper I, υ And and τ Boo, along with ρ CrB make up the Group 2 stars.

For the purpose of studying line profile shapes, additional spectra were obtained at the author's request by David Lambert and Eric Bakker using the 2.7 m telescope at McDonald observatory equipped with the coudé echelle (Tull et al.) giving a resolving power (depending on the slit width) near 230,000 for 47 UMa, 70 Vir, and HD 114762, 180,000 for ρ^1 Cnc, and 115,000 for 51 Peg; the S/N ratios are in the range of 250 to 350, except for HD 114762, which is near 200. The spectral coverage is 4700 - 5800 Å for 47 UMa, 70 Vir and HD 114762 and 5700 - 7900 Å for 51 Peg with significant gaps between orders; the high-resolution spectra only cover about 20 Å per order, and the orders are separated by about 100 Å. Each observation was broken up into two or three exposures in order to detect and eliminate cosmic ray hits. The procedures followed in reducing all the spectra are the same as those described in Gonzalez & Lambert (1996) and in Paper I.

3. Analysis

3.1. Abundance analysis

Our method of abundance analysis closely follows that used in Paper I and by Gonzalez & Lambert in their study of several stars in the α Per cluster. Like those studies, this analysis is a differential one with respect to the Sun. Since the stars on our program are similar to the Sun in their physical characteristics, a differential abundance analysis with the Sun as the source of the gf-values (as opposed to laboratory gf-values) avoids many possible systematic errors. These include uncertainties in the treatment of the structure of the atmospheres, such as differences in the mixing length to scale height ratio or convection and chromospheric activity, especially starspots.[2] Following Paper I

[1] Group 1 includes ρ^1 Cnc, 16 Cyg A and B, 51 Peg, 47 UMa, 70 Vir, and HD 114762.

[2] Sunspots and starspots may vary on a monthly or yearly basis. Also, the area covered by starspots averaged over a starspot cycle may vary from star to star; this may be a problem for solar type stars younger than the Sun, which typically display stronger chromospheric activity. However, this is not the case for our program stars, which have low chromospheric activity.

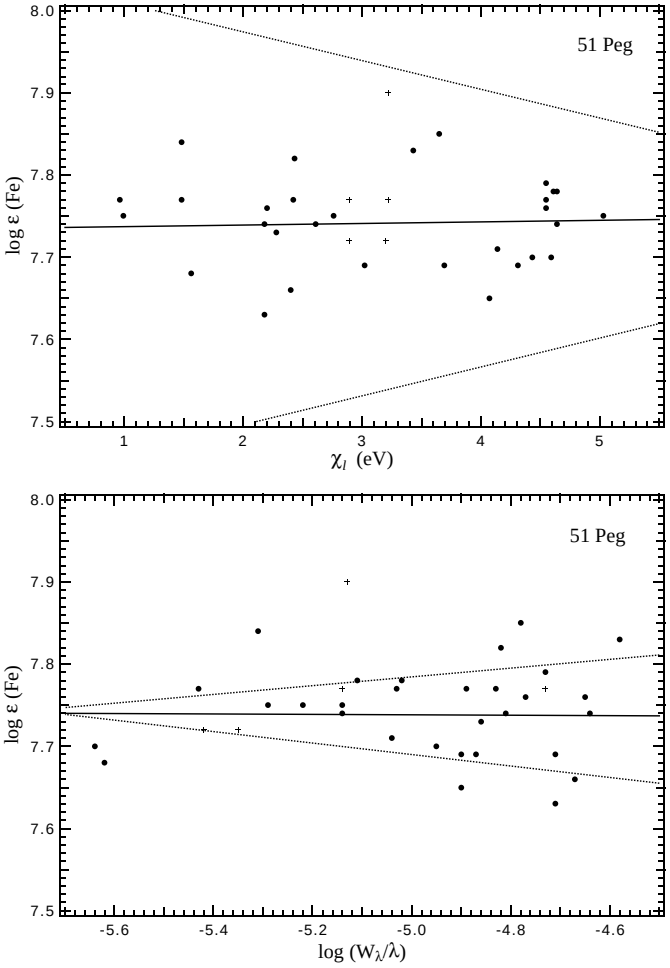

Fig. 1. The Fe I (filled circles) and Fe II (plus signs) abundances calculated using the model parameters given in Table 3 are plotted versus $\chi_{\rm l}$ and $\log(W_\lambda/\lambda)$. The solid lines are least-squares fits through the Fe I data points. The dotted lines in the first diagram are the least-squares fits when $T_{\rm eff}$ is changed by $\pm$ 250 K. The dotted lines in the second diagram are the least-squres fits when $\xi_{\rm t}$ is changed by $\pm$ 0.2 km s^{-1}.

and Gonzalez & Lambert we employ the Kurucz (1993) model atmospheres; the effective temperature, $T_{\rm eff}$, surface gravity, g, and depth-independent microturbulence parameter, $\xi_{\rm t}$, are estimated in the standard way using the Fe I and Fe II lines (details are discussed in Sect. 3.1.1).

The abundance analyses of the Group 1 stars are based on measurements of the moderate resolution spectra obtained with the 2.1 m telescope, while the analysis of ρ CrB is based on the moderate resolution spectrum obtained with the 2.7 m. The spectral lines used in the present analysis were selected from the linelist in Tables 12 and 13 of Gonzalez & Lambert and Table 1 of Paper I. Additional lines were added in the analysis of the Group 1 stars (Table 1) and their gf-values estimated using the equivalent widths (W_λ's) measured on the Solar Flux Atlas (Kurucz et al. 1984); additional lines in the analysis of ρ CrB (Table 2) are based on measurements of a spectrum of Vesta described in Paper I. Although the wavelength coverage is quite extensive and the quality of the spectra is very high, we have been very restrictive in our selection of lines for use in the abundance analysis. To be suitable, a spectral line must be unblended (except for the few rare instances where the line is critical to estimating the abundance of a given element) and have a symmetric profile in both the target star spectrum and the solar spectrum. The sample is restricted to mostly moderate strength lines with W_λ's between about 10 and 150 mÅ (weaker lines have a larger relative error in the W_λ measurements due to noise, and stronger lines are more sensitive to errors in $\xi_{\rm t}$). Comparing measurements of the same lines on spectra taken on different nights, we estimate that the average uncertainty in an W_λ measurement to be about 1-2 mÅ for lines with W_λ near 50 mÅ and about 2-3 mÅ for stronger ones. Such low errors were achieved by smoothing isolated lines (effectively increasing the S/N ratio), measuring some lines on the overlap regions of adjacent orders, and averaging W_λ measurements from spectra obtained on different observing runs.

3.1.1. Model atmosphere selection and Fe abundances

While hundreds of Fe lines are present in the spectral regions observed, we selected only 30 Fe I and 5 Fe II for use in the analysis (the total number varies from star to star). The values of $T_{\rm eff}$, $\log g$, $\xi_{\rm t}$, and [Fe/H] have been estimated for each star (Table 3) with this sample of Fe lines using an updated version of the LTE line abundance code, MOOG (Sneden 1973). The atmospheric parameters are determined with an iterative procedure. We begin with an initial set of parameters equal to those determined in previous studies. All four parameters are adjusted in a systematic manner until the correlation coefficients between $\log\epsilon$(Fe I) and $\xi_{\rm t}$ and between $\log\epsilon$(Fe I) and $\log(W_\lambda/\lambda)$ are zero and also $\log\epsilon$(Fe I) = $\log\epsilon$(Fe II). The range of the measured Fe I line strengths is sufficient to estimate $\xi_{\rm t}$ accurately. We note that the values of $\xi_{\rm t}$ we derived for all the stars but ρ^1 Cnc and ρ CrB are the same as the solar value, as expected. The range of the lower excitation potentials, $\chi_{\rm l}$, is 1.0 to 5.0 eV for the Fe I lines, which is sufficient to estimate $T_{\rm eff}$ accurately for each of the program stars. The typical uncertainties of our estimates of $T_{\rm eff}$, $\log g$, and $\xi_{\rm t}$ are 75 K, 0.1, and 0.1 km s^{-1}, respectively (individual values are listed in Table 3). They lead to a typical uncertainty in [Fe/H][3] of 0.06 dex, which was calculated with the sensitivities of the abundances to changes in atmospheric parameters (Table 5). The sensitivities of the $\log\epsilon$(Fe) versus $\chi_{\rm l}$ and $\log\epsilon$(Fe) versus $\log(W_\lambda/\lambda)$ relationships to changes in $T_{\rm eff}$ and $\xi_{\rm t}$, respectively, are shown in Fig. 1 for 51 Peg. The measured values of W_λ for each line are listed in Table 4.

As a check on the estimated uncertainties in the atmospheric parameters, we note that the removal of three high-weight Fe I lines (at 6574 Å, 6581 Å, and 6591 Å; all have small values of W_λ and two have low values of $\chi_{\rm l}$) from the analysis resulted in revisions to the atmospheric parameters within the range of

[3] Throughout the present work we use the standard spectroscopic notation, $[X/Y] \equiv \log_{10}[N_{\rm X}/N_{\rm Y}]_{\rm star} - \log_{10}[N_{\rm X}/N_{\rm Y}]_\odot$, where $N_{\rm X}$ and $N_{\rm Y}$ represent the number density abundances of elements X and Y. We also employ the relation, $\log\epsilon(X) = \log_{10}(N_{\rm X}/N_{\rm H}) + 12.0$.

Table 3. Atmospheric parameters derived from the Fe-line analyses

Star	HR	HD	$T_{\rm eff}$(K)	$\log g$	$\xi_{\rm t}$(km s^{-1})	[Fe/H]	N(Fe I, Fe II)
ρ^1 Cnc	3522	75732	5150 ± 75	4.15 ± 0.05	0.8 ± 0.10	0.29 ± 0.06	19, 6
ρ CrB	5968	143761	5750 ± 75	4.10 ± 0.05	1.2 ± 0.10	-0.29 ± 0.06	25, 5
16 Cyg A	7503	186408	5750 ± 75	4.20 ± 0.05	1.0 ± 0.10	0.11 ± 0.06	28, 3
16 Cyg B	7504	186427	5700 ± 75	4.35 ± 0.05	1.0 ± 0.10	0.06 ± 0.06	28, 3
51 Peg	8729	217014	5750 ± 75	4.40 ± 0.10	1.0 ± 0.10	0.21 ± 0.06	30, 5
47 UMa	4277	95128	5800 ± 75	4.25 ± 0.05	1.0 ± 0.10	0.01 ± 0.06	26, 5
70 Vir	5072	117176	5500 ± 75	3.90 ± 0.10	1.0 ± 0.10	-0.03 ± 0.06	25, 4
HD 114762	—	114762	5950 ± 75	4.45 ± 0.05	1.0 ± 0.10	-0.60 ± 0.06	17, 3

The adopted values of $T_{\rm eff}$, $\log g$, and $\xi_{\rm t}$ have been rounded to within 50 K, 0.05, and 0.1 km s^{-1}, respectively.

the uncertainties. The only exception is ρ^1 Cnc, for which the change in $\log g$ was significantly larger than the estimated uncertainty in this parameter; this was due to the small number of Fe I lines (especially weak lines) measured in its spectrum. Overall, though, this shows that our solutions are robust and consistent with the quoted uncertainties. Finally, we should note that although our method of analysis closely follows that of Gonzalez & Lambert, our results are more precise than theirs due to our use of Fe I lines with a larger spread in W_λ and χ_1. Also, our results are more precise than those of Paper I due to the lower rotation velocities of our sample.

3.1.2. Other elements

Since the resonance line of lithium is blended with other lines in spectra of solar-type stars, we must employ spectrum synthesis methods to estimate its abundance. We used the linelist of Cunha et al. (1995, Table 7), modified slightly to reproduce the solar spectrum using the Kurucz solar model atmosphere; the spectral region synthesized spans 6700 to 6711 Å. The same stellar atmospheric parameters derived from the Fe-line analysis were used in producing the synthetic spectra. The line broadening was approximated with a Gaussian function with a width chosen so that the two strongest Fe I lines in the observed spectra are reproduced accurately. The lithium line is discernible by eye on all spectra, except those of ρ^1 Cnc and 16 Cyg B, where it is not detectable at the level of the noise. Sample spectra and syntheses of the Li I region are shown in Fig. 2a and b for 16 Cyg A and B, for which we derive very different lithium abundances.

The abundances of 15 additional elements were determined with the atmospheric parameters listed in Table 3. The individual line measurements are listed in Table 4, and the final abundances are given in Tables 6,7,8. As in the Fe abundance analyses, the uncertainties in the [X/H] values were calculated with the estimated uncertainties in the atmospheric parameters (Table 3) and the data in Table 5.

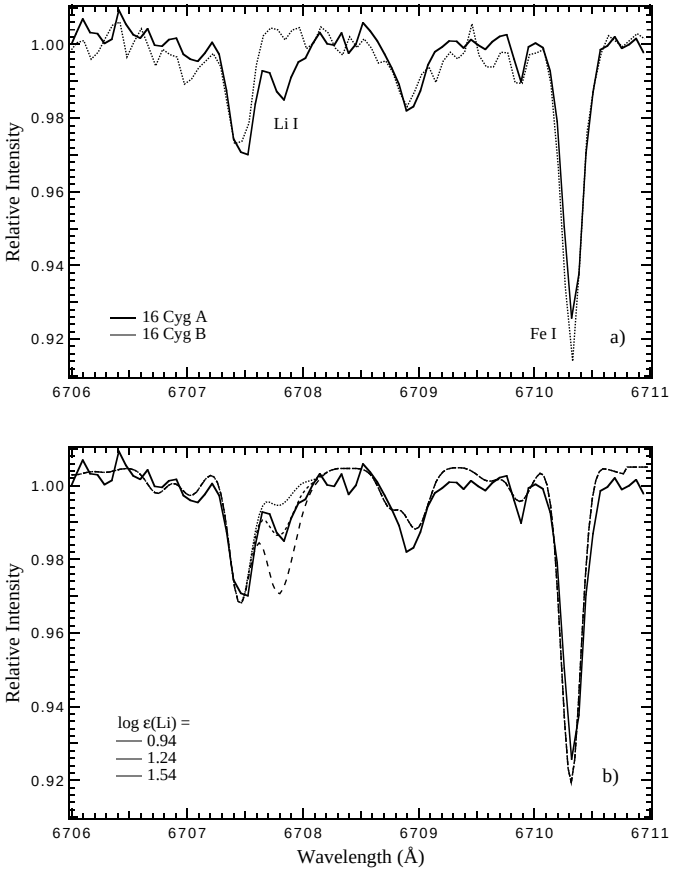

Fig. 2a and b. Portions of the spectra of 16 Cyg A and B containing the Li I line at 6707.8 Å (panel **a**). The strength of the Li I line differs significantly on the two spectra. Each spectrum is the average of three spectra obtained on different nights. The resultant S/N ratios are near 350. Shown in panel **b** is a comparison of a spectrum of 16 Cyg A with three syntheses, each differing only in the lithium abundance assumed.

3.2. $v \sin i$

To estimate the masses of the claimed planetary mass companions, we require, among other quantities, estimates of their orbital inclinations. Assuming that the orbital axis of a planet is aligned with the rotation axis of its parent star, an estimate of the projected stellar rotational velocity ($v \sin i$) can be used to constrain the orbital inclination. In the following we describe the derivation of $v \sin i$ for ρ^1 Cnc, 51 Peg, 47 UMa, 70 Vir, HD 114762 from high-resolution spectra (obtained with the 2.7 m

Table 4. Equivalent widths of the program stars

Element Wavelength(Å)	ρ^1 Cnc	ρ CrB	51 Peg	47 UMa	70 Vir	HD 114762	16 Cyg A	16 Cyg B
C I								
5380.31	21	19.4	28	24	22	10		
6587.62		12.1	17	17	13		19	17
O I								
7771.94		80.8	89	89	61		84	81
7774.16		69.2	75	83	53		73	72
7775.38		57.5	64	71	45		59	55
Na I								
5688.20			150	129	122	72		
6154.23	98	26.4	57					
6160.75	117		71					
Mg I								
5711.08		98.5	125	107	112	75	114	112
Al I								
6698.65	67		36					
7835.29		39.2	68	39	58		58	58
7836.11		52.7	84	54	65		70	68
Si I								
5793.06	69	37.7	57	46	50	22	52	51
5948.54			102					
6125.41		30.5						
6145.41		33.2						
6721.85		38.9	67	49	44	21	55	54
S I								
6052.65		11.7	18	17			18	14
Ca I								
5867.55	59	19.5	32	24	26		31	27
6166.44		63.2						
6455.59	99		70		62	26	64	64
6471.65			102	94	104		100	100
Sc II								
5526.80		80.9	91	86	89	61	87	83
6604.58		38.1	50	42	48	20	47	44
Ti I								
6126.21	71	19.2	36	23	35	8	55	56
6261.09		43.3	63	48	63	24		
Ti II								
5336.78		77.6	80		83	66		
5418.77	55	57.0	57		60	63		
Cr I								
5783.07	67		43	31	39		34	33
5783.87	89		61	44	54	11	50	44
Fe I								
5044.21		64.2						
5288.52			71	59	63	27		
5322.04		50.6	73	63	70	24		
5560.21	76		63	52	58	20	58	57
5576.09			145	120	127	74	124	127
5806.73		41.8						
5852.22		29.0						
5855.09		14.7						
5856.10		24.1						
5859.57	107		86	76	77	34	76	78
5862.35	130		108	87	89	48	94	96

Table 4. (continued) Equivalent widths of the program stars

Element Wavelength(Å)	ρ^1 Cnc	ρ CrB	51 Peg	47 UMa	70 Vir	HD 114762	16 Cyg A	16 Cyg B
6024.06		93.0	135	110	119	66	119	120
6027.05	88	56.8	76	64	71	28	69	68
6056.01		61.1						
6065.48		103.7	139	119	129	80	122	122
6089.56	63							
6093.63	54							
6151.62		38.8						
6165.36	69	34.1	56					
6213.43	122	74.3						
6232.63			104				90	93
6252.57			134		129	75	131	130
6265.14		77.2	98	86	95		95	95
6335.34			108	97	116	63	104	105
6380.74		41.8						
6430.85			126	111	122	75	121	121
6498.94	88	34.8	60	47	62	14	53	56
6574.25	73		40	29	42	6	32	35
6581.22	58		32	20	29		27	27
6591.33	30	5.3	15	11	12		15	14
6593.87	128		99	83	92	45	93	93
6703.55	65	27.8	49	34	50	9	43	42
6710.30		10.5	25	16	29		18	19
6733.15		17.5	25	16	29		18	19
6739.51	40	7.2	16	10	17		14	15
6750.15	112	66.0	87	73	82		80	81
6752.70		25.1	49	34		14	43	43
6806.84	70						40	40
6810.26	81		65				58	56
6820.36	75		53	41			48	49
7583.78		76.1	96	82	95		90	91
7586.01		103.5	147	128	123		136	140
7588.29			39	27	33		31	34
Fe II								
5234.62	78	80.7	97	88	83	67		
5414.08	34		40	31	34	13		
5991.38		37.0						
6084.10	19		27	25	27		29	26
6149.25	35	35.4						
6369.45		19.0	24	23			24	21
6247.56	49							
6432.68	43		47	46	49	23	50	45
Co I								
6454.98	43		25		18		17	18
6814.96			30				28	27
Ni I								
5082.34			82			30		
6767.76	115	72.0	92	80	88	46	84	86
Y II								
4883.69						41		
5087.42				52	52	25		
Zn I								
4722.15		70.1						
Ba II								
5853.67	75	61.6	71	73	70	39	71	70

Table 5. Sensitivities of calculated abundances to changes in model atmosphere parameters for 51 Peg and ρ^1 Cnc

Star Line,λ(Å),W_λ(mÅ)	$\Delta T_{\rm eff} =$ +250 K	$\Delta \log g =$ +0.5(cgs)	$\Delta\xi_{\rm t} =$ +0.5 km s^{-1}	$\Delta W_\lambda =$ +2%
51 Peg				
O I, 7774.16, 75	−0.24	+0.10	−0.05	+0.03
Ca I, 6455.59, 70	+0.18	−0.07	−0.10	+0.03
Sc II, 6604.58, 50	−0.01	+0.21	−0.10	+0.02
Fe I, 6750.15, 87	+0.21	−0.06	−0.20	+0.03
Fe I, 7588.29, 39	+0.10	−0.02	−0.05	+0.02
Fe II, 6432.68, 47	−0.11	+0.22	−0.10	+0.02
Fe I (all)	+0.19	−0.07	−0.13	+0.02
Fe II (all)	−0.07	+0.20	−0.10	+0.01
ρ^1 Cnc				
C I, 5380.31, 21	−0.25	+0.18	−0.01	+0.01
Ca I, 6455.59, 99	+0.23	−0.15	−0.17	+0.03
Ti II, 5418.77, 55	−0.03	+0.19	−0.14	+0.02
Fe I, 6591.33, 30	+0.05	+0.04	−0.04	+0.02
Fe I, 6750.15, 112	+0.18	−0.08	−0.26	+0.03
Fe II, 6432.68, 43	−0.22	+0.25	−0.12	+0.02
Fe I (all)	+0.13	−0.04	−0.16	+0.02
Fe II (all)	−0.21	+0.23	−0.12	+0.01

Table 6. Final adopted abundances for ρ^1 Cnc, 51 Peg, 47 UMa, 70 Vir, and HD 114762

Element	$\log \epsilon_\odot$	ρ^1 Cnc [X/H]	N	51 Peg [X/H]	N	47 UMa [X/H]	N	70 Vir [X/H]	N	HD 114762 [X/H]	N
Li	1.06	< -1.1	1	0.44±0.10	1	0.65±0.10	1	0.70±0.10	1	1.20±0.10	1
C	8.55	0.31±0.10	1	0.12±0.07	2	0.00±0.09	2	0.01±0.07	2	−0.51±0.09	1
O	8.94			0.24±0.08	3	0.22±0.08	3	0.00±0.08	3		
Na	6.34	0.32±0.08	2	0.18±0.08	3	0.15±0.08	1	0.03±0.10	1	−0.41±0.08	1
Mg	7.61			0.15±0.09	1	−0.01±0.09	1	−0.04±0.10	1	−0.39±0.08	1
Al	6.51	0.50±0.09	1	0.29±0.07	3	−0.04±0.08	2	0.09±0.06	2		
Si	7.58	0.42±0.09	1	0.21±0.08	3	0.04±0.05	2	−0.04±0.08	2	−0.43±0.06	2
S	7.29			0.22±0.10	1	0.14±0.10	1				
Ca	6.37	0.29±0.07	2	0.16±0.08	3	0.05±0.07	2	−0.03±0.07	3	−0.47±0.08	1
Sc	3.11			0.33±0.07	2	0.06±0.05	2	0.05±0.05	2	−0.48±0.04	2
Ti	4.96	0.24±0.08	2	0.24±0.06	4	0.05±0.06	2	0.03±0.07	4	−0.31±0.08	4
Cr	5.71	0.36±0.09	2	0.25±0.07	2	0.01±0.06	2	0.01±0.07	2	−0.73±0.08	1
Fe	7.53	0.29±0.06	22	0.21±0.06	35	0.01±0.06	31	−0.03±0.06	29	−0.60±0.06	20
Co	4.93	0.49±0.08	1	0.30±0.06	2			−0.07±0.09	1		
Ni	6.27	0.34±0.10	1	0.31±0.07	2	0.04±0.09	1	−0.05±0.09	1	−0.55±0.07	2
Y	2.25					−0.05±0.08	1	−0.22±0.08	1	−0.68±0.10	2
Ba	2.23	0.24±0.09	1	0.17±0.08	1	0.13±0.08	1	−0.12±0.08	1	−0.80±0.07	1

The uncertainties in [X/H] are a combination of the random (line-to-line) and systematic (uncertainties in atmospheric parameters) error sources. The quoted solar lithium abundance is that of the photosphere. The other solar abundances are from Gonzalez & Lambert (1996).

telescope) and for ρ CrB from a moderate-resolution spectrum. In addition to the program star spectra, a spectrum of the sky was acquired to calibrate our technique with the known solar parameters.

We employ the Fourier transform method, supplemented by line profile synthesis, to estimate $v \sin i$ from the stellar spectra. The instrumental, macroturbulent ($\zeta_{\rm RT}$), microturbulent, rotational, and thermal broadening mechanisms are included in the analysis of a given line profile. The syntheses have been carried out with MOOG, which includes all the line broadening mechanisms; as in the abundance analysis, we make use of the Kurucz (1993) LTE model atmospheres. We have adopted the radial-

Table 7. Final adopted abundances for 16 Cyg A and B

Element	16 Cyg A [X/H]	16 Cyg B [X/H]	N
Li	0.18±0.10	< -0.6	1
C	0.14±0.10	0.15±0.10	1
O	0.13±0.08	0.17±0.08	3
Mg	0.08±0.09	−0.02±0.09	1
Al	0.18±0.06	0.12±0.07	2
Si	0.12±0.07	0.09±0.07	2
S	0.16±0.09	0.09±0.09	1
Ca	0.14±0.07	0.05±0.07	3
Sc	0.15±0.04	0.13±0.04	2
Ti	0.12±0.08	0.08±0.08	1
Cr	0.07±0.08	0.01±0.08	2
Fe	0.11±0.06	0.06±0.06	31
Co	0.14±0.08	0.12±0.08	2
Ni	0.08±0.09	0.06±0.09	1
Ba	0.09±0.08	0.08±0.08	1

Table 8. Final adopted abundances for ρ CrB

Element	$\log \epsilon_{\odot}$	[X/H]	N
Li	1.06	0.24±0.10	1
C	8.56	−0.18±0.09	2
O	8.94	0.06±0.08	3
Na	6.33	−0.23±0.09	1
Mg	7.58	−0.15±0.09	1
Al	6.47	−0.03±0.06	2
Si	7.55	−0.13±0.06	4
S	7.21	−0.11±0.10	1
Ca	6.36	−0.13±0.07	2
Sc	3.10	−0.17±0.06	2
Ti	4.99	−0.15±0.06	4
Fe	7.47	−0.29±0.06	30
Ni	6.25	−0.29±0.09	1
Zn	4.60	−0.25±0.09	1
Ba	2.23	−0.42±0.08	1

tangential description of macroturbulent line broadening (Gray 1992), and we have approximated the instrumental broadening by a Gaussian function, its width determined from the emission lines in the Th-Ar comparison spectrum obtained immediately following each stellar observation. This approximation is a very close fit to the Th-Ar lines; however, even if it were not, it would not cause significant errors since the instrumental broadening is minor compared to the other line broadeners. The limb darkening coefficients, required for synthesizing the rotational profiles, have been interpolated from Fig. 17.6 of Gray (1992). The model atmosphere parameters used in the syntheses are the same as those estimated from the Fe-line analyses in Sect. 3.1.1, except for the Fe abundance and $\xi_{\rm t}$ (see below).

The Fe I lines at $\lambda\lambda$ 5379.586, 5638.249, 5731.762 Å were selected for analysis from Table 2 of Takeda (1995); these lines are unblended, moderate in strength, and have smaller than average and nearly identical $\zeta_{\rm RT}$ values. Our high-resolution spectrum of 51 Peg did not include these lines, since it was obtained with a different instrumental setup; we used the Fe I lines at $\lambda\lambda$ 6200.313, 6213.430, 6322.686 Å instead. All the lines selected for analysis appear symmetric upon visual inspection and do not have any other lines within about 0.3 Å of their line cores. The spectra were shifted to the rest frame and 0.6 Å sections containing the Fe I lines were isolated for further analysis. Each section contains the entire line profile along with a small amount of continuum.

The analysis method involves first producing a synthesis of a line and manually adjusting the values of $v \sin i$, $\zeta_{\rm RT}$, $\log \epsilon$(Fe), and the continuum level until the residuals between it and the observed profile are minimized. Next, the Fourier amplitude spectrum of the observed profile is compared with the Fourier amplitude spectra of synthetic line profiles using a range of $v \sin i$ and $\zeta_{\rm RT}$ values centered on the best-fit set. The synthetic profiles are generated by convolving the instrinsic stellar thermal profile with the instrumental, microturbulent, macroturbulent, and rotational broadening functions. We analyzed the solar spectrum first with $v \sin i$ set equal to 1.7 km s^{-1} ($v \sin i$ is the synodic rotation velocity of the Sun; Soderblom 1982) in order to estimate $\xi_{\rm t}$ and $\zeta_{\rm RT}$. The value of $\xi_{\rm t}$ required to reproduce the solar Fe I line profiles is 0.4 km s^{-1}. In their studies of the solar spectrum Gray (1977) and Takeda (1995) find that they must assume $\xi_{\rm t}$ = 0.5 km s^{-1} in order to reproduce the line profiles accurately. This is half the value we used in our abundance analyses of solar Fe I lines. The discrepancy is likely caused by the approximate nature of our line profile synthesis method and model-incompleteness (see Takeda et al. 1996 for a brief discussion of this problem). Regardless of its source, it is only a scientific problem, not a practical one. Both Soderblom (1982) and Hale (1995) find that $v \sin i$ is only weakly dependent upon $\xi_{\rm t}$.

Treating both $v \sin i$ and $\zeta_{\rm RT}$ as free parameters and fixing $\xi_{\rm t}$ at 0.4 km s^{-1}, we obtain $\zeta_{\rm RT} = 3.5 \pm 0.2$ and $v \sin i = 1.6 \pm 0.2$ km s^{-1} for the solar lines.[4] The final step in the analysis involves comparing the synthetic line profile with the observed profile again, this time using the parameters determined from the Fourier analysis. To obtain an adequate fit to observed solar line profiles, it was found necessary to increase $\log \epsilon(Fe)$ by 0.05 dex and $v \sin i$ by 0.1 km s^{-1}. We followed the same procedure in analyzing the line profiles of the other stars. We present the final results in Table 9 and sample Fourier amplitudes and synthetic spectra in Figs. 3 and 4, respectively. The quality of the spectra vary considerably, with those of the Sun, 70 Vir, and 47 UMa being the best and HD 114762 the poorest. The quality of the 51 Peg profiles is quite high, but the resolving power is only half that of the best spectra. The resolving power of the ρ^1 Cnc spectrum is intermediate between that of 51 Peg

[4] We note that our estimates of $\zeta_{\rm RT}$ for the solar Fe I lines (3.5 km s^{-1}) is greater than the value quoted by Takeda for the same lines by about 0.3 km s^{-1}; this is likely due to Takeda's adoption of an incorrect value of $v \sin i$ in his analysis (1.9 instead of 1.7 km s^{-1}).

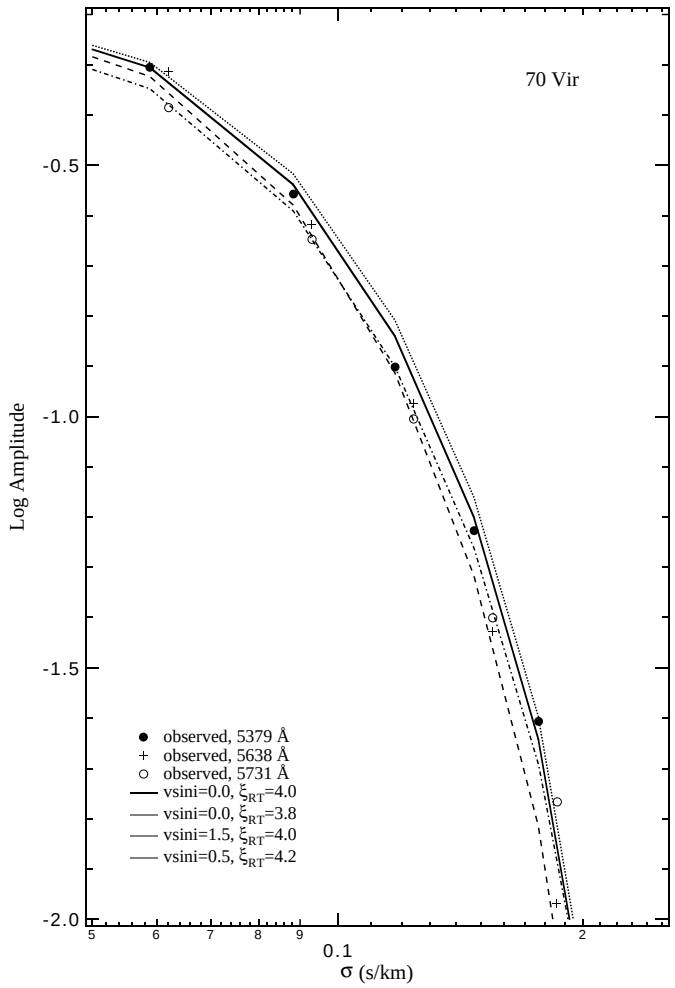

Fig. 3. Fourier transforms of three Fe I lines in the high-resolution spectrum of 70 Vir. Also shown are the theoretical transforms calculated using different combinations of $v \sin i$ and $\zeta_{\rm RT}$.

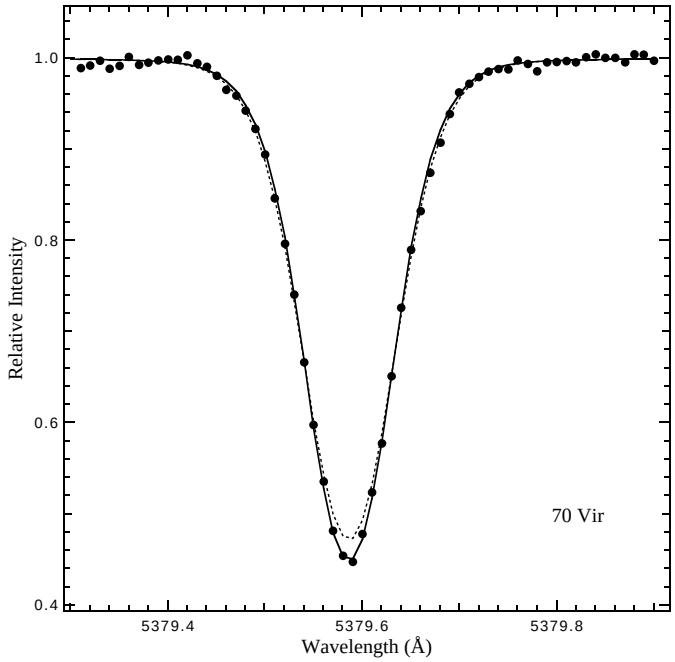

Fig. 4. Synthetic profile (solid curve) of the Fe I line at 5379.59 Å in the spectrum of 70 Vir using $\zeta_{\rm RT}$ = 4.2 and $v \sin i$ = 0.5 km s^{-1}; the dashed curve corresponds to $\zeta_{\rm RT}$ = 4.2 and $v \sin i$ = 1.5 km s^{-1}.

and the other stars, but given that it is much cooler than the other stars and very metal-rich, the continuum is not nearly as smooth due to the presence of weak lines, which mimic noise. Zeeman broadening was not included in any of the analyses, since it has not been found to be a significant source of line broadening for stars hotter that G6 (Gray 1984). The low chromospheric activity of ρ^1 Cnc implies that Zeeman broadening is probably not significant for this star, even though its spectral type is G8.

We have calculated the expected value of $\zeta_{\rm RT}$ for each star based on the relation between it and the fundamental stellar parameters, as given in Gray (1992). Using Gray's (1992) Fig. 18.9 and the results of Gray (1984), we have generated an interpolation equation relating $\zeta_{\rm RT}$ to $T_{\rm eff}$ and $M_{\rm V}$ and another relating $\zeta_{\rm RT}$ to $T_{\rm eff}$ and $\log g$, with residuals of $\pm$ 0.2 and $\pm$ 0.5 km s^{-1}, respectively:

$$\zeta_{\rm RT}(M_{\rm V}) = -9.71 + 3.18(T_{\rm eff}/1000) - 0.66 M_{\rm V} - 0.07(T_{\rm eff}/1000) M_{\rm V} \quad (1)$$

$$\zeta_{\rm RT}(g) = -44.55 + 11.13(T_{\rm eff}/1000) + 9.28 \log g - 2.24(T_{\rm eff}/1000) \log g \quad (2)$$

The zero points of these equations were set such that they yield the value of $\zeta_{\rm RT}$ that we estimated for the Sun (Table 9). The predicted values of $\zeta_{\rm RT}$ are consistent with the measured values, except for ρ^1 Cnc, where the two predicted values are very different from each other.

We should note that the uncertainties we quote are formal. They are based on the scatter of the solutions for the individual lines. We have not taken into account possible systematic errors caused by velocity fields not included in our line modeling. The upper limits are also formal. The upper limit for 70 Vir is more secure than for ρ^1 Cnc and HD 114762 due to the small scatter among the Fourier amplitude plots of the observed spectra. The extreme upper limit of $v \sin i$ allowed by the data for 70 Vir is somewhat short of 1 km s^{-1}, while for ρ^1 Cnc and HD 114762 it might approach 2 km s^{-1}. The close agreement between the predicted and measured values of $\zeta_{\rm RT}$ for all the stars but ρ^1 Cnc is encouraging.

Due to the lower resolving power of our spectrum of ρ CrB, we did not attempt to determine both $\zeta_{\rm RT}$ and $v \sin i$ for this star. Instead, we fixed $\zeta_{\rm RT}$ at 4.2 km s^{-1} from Eqs. 1 and 2. Using only the spectrum synthesis method with the 5379 and 5638 Å Fe I lines, we determined the best-fitting value of $v \sin i$ to be about 1.5 km s^{-1}.

Previous estimates of $v \sin i$ exist for all our program stars. The quality of these estimates varies considerably depending on the quality of the spectra (due both to resolving power and S/N ratio), the number of lines analyzed, and the method used (line synthesis or Fourier transform); it seems that every work adopts a different approach in estimating $v \sin i$. We list in Table 10 the published $v \sin i$ values. We also list in the table the mean

Table 9. Predicted $\zeta_{\rm RT}$ and measured $\zeta_{\rm RT}$ and $v \sin i$ values

Star	$\zeta_{\rm RT}(M_{\rm V})$ (km s^{-1})	$\zeta_{\rm RT}(g)$ (km s^{-1})	$\zeta_{\rm RT}$(meas.) (km s^{-1})	$v \sin i$ (km s^{-1})
Sun	—	—	3.5±0.2	1.7±0.2
ρ^1 Cnc	1.1	3.4	3.2±0.4	< 1.3
51 Peg	3.8	3.6	3.9±0.2	1.4±0.3
47 UMa	4.2	4.3	4.2±0.2	1.7±0.4
70 Vir	4.0	4.8	4.1±0.1	< 0.5
HD114762	4.7	3.7	4.0±0.4	< 1.5
ρ CrB	4.1	4.6	—	∼1.5

The values of $\zeta_{\rm RT}$ listed in columns 2 and 3 were calculated using Eqs. 1 and 2, respectively. ρ CrB was analyzed in a different way from the other stars - see text for details.

Table 10. Published estimates of $v \sin i$ and mean adopted values

Star	$v \sin i$ (km s^{-1})	Reference	adopted $v \sin i$ (km s^{-1})
ρ^1 Cnc	1.9±1.0	Baliunas et al. (1997)	< 1.5
ρ CrB	1.5±1.0	Soderblom (1982)	1.5±0.5
16 Cyg B	2.7±1.0	Soderblom (1982)	2.7±1.0
51 Peg	2.1±0.6	Baranne et al. (1979)	
	1.7±0.8	Soderblom (1982)	
	2.8±0.5	Mayor & Queloz (1995)	
	2.4±0.3	Francois et al. (1996)	
	2.35±0.1	Hatzes et al. (1997)	2.1±0.4
47 UMa	2.8±0.7	Soderblom (1982)	
	1.9±0.6	Henry et al. (1997)	2.1±0.5
70 Vir	0.9±0.4	Henry et al. (1997)	< 0.5
HD114762	0^{+1}_{-0}	Cochran et al. (1991)	
	0.8±0.7	Hale (1995)	< 1

Note - The quoted values of $v \sin i$ for 51 Peg by Francois et al. (1996) and Hatzes et al. (1997) have each been reduced by 0.2 km s^{-1} in deriving the adopted value. See the text for details.

adopted values giving all estimates equal weight and correcting Hatzes et al.'s (1997) and Francois et al.'s (1996) estimates by -0.2 km s^{-1}. Hatzes et al. incorrectly used a solar $v \sin i$ value of 2.0 km s^{-1} in calibrating their method, and Francois et al. incorrectly assumed the value of $\zeta_{\rm RT}$ in 51 Peg is the same as in the Sun.

4. Discussion

4.1. Abundances

All our program stars are listed in the catalog of Cayrel de Strobel et al. (1997), which is a compilation of stellar spectroscopic [Fe/H] determinations from the published literature up through the end of 1995. They list seven estimates for HD 114762 ranging from -0.59 to -0.87. For the other stars the [Fe/H] estimates are as follows: ρ^1 Cnc has four ranging from -0.15 to $+0.30$; ρ CrB has four ranging from -0.26 to -0.14; 16 Cyg A has four ranging from 0.00 to 0.22, and 16 Cyg B has five ranging from 0.00 to 0.11; 51 Peg has three ranging from 0.06 to 0.12; 47 UMa has two, -0.02 and 0.01; 70 Vir has one at -0.11.

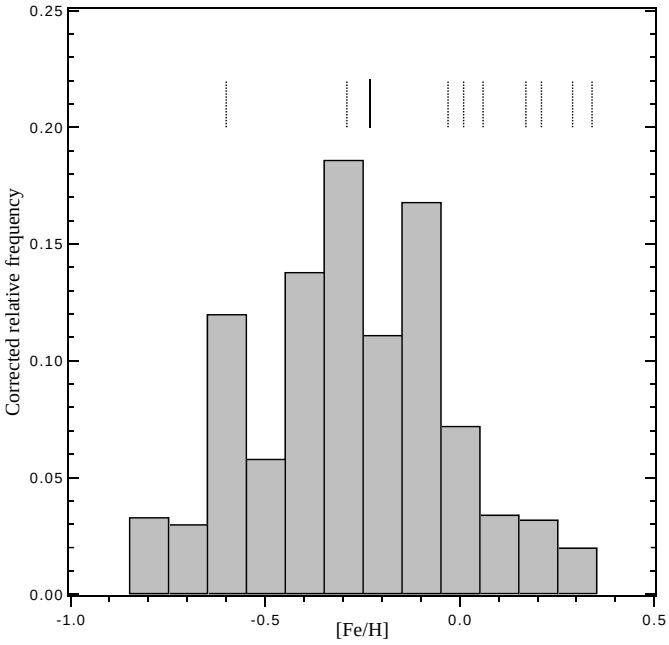

Fig. 5. Histogram of the distribution of spectroscopic [Fe/H] estimates for nearby G dwarfs (with $T_{\rm eff} > 5100$ K; 66 stars) from Favata et al. (1997). The average value of the distribution is indicated with a solid vertical line and our [Fe/H] estimates by dotted vertical lines (the two stars from Paper I are also included). Favata et al. have corrected their distribution for scale Galactic height inflation.

There are a few more recent spectroscopic studies that have included some of our program stars. Tomkin et al. (1997) have recently reanalyzed the "NaMgAl" stars, originally noted in the Edvardsson et al. (1993) study. Using higher quality spectra, they now conclude that this group was spurious. Included in this group was 51 Peg, for which they now derive [Fe/H] = 0.20 ± 0.07. Feltzing & Gustafsson (1998) derive [Fe/H] = 0.06 for 16 Cyg B. Fuhrmann et al. (1997) derive [Fe/H] = 0.20 ± 0.07 and 0.00 ± 0.07 for 51 Peg and 47 UMa, respectively. All these determinations are very close to ours.

In his study of super metal-rich (SMR; defined as having [Fe/H] > 0.2 with ≥95% confidence) stars, Taylor (1996) lists 29 luminosity class IV-V candidates (his Table 4). He includes ρ^1 Cnc and 51 Peg in this list, for which he quotes photometric [Me/H] estimates of $+0.5$ and $+0.25$, respectively. Mean spectroscopic [Fe/H] values, based on published estimates and transformed to a uniform temperature and metallicity scale by him, are 0.41 ± 0.10 and 0.17 ± 0.05, respectively. While having two of our program stars appear in a list of 29 suspected SMR stars seems significant, it becomes less so when it is noted that 10 of the 120 stars analyzed by Marcy and Butler's group also appear on the list. More significant, however, is the fact that Taylor lists ρ^1 Cnc as one of the 7 stars with a probability ≥ 95% of being a SMR star; none of the other stars observed by Marcy & Butler's group is a member of this "magnificent seven." In Paper I we derived [Fe/H] values for υ And and τ Boo of 0.17

$\pm$ 0.08 and 0.34 $\pm$ 0.09, respectively. These results, combined with those of Boesgaard & Lavery (1986), compel us to add τ Boo to this select group of nearby SMR stars.

More recently, Feltzing & Gustafsson (1998) have performed spectroscopic abundance analyses on 47 G and K stars with [Me/H] > 0.00. They sample a larger volume of space, going down to $m_{\rm v}$ = 9.15, and find seven stars with [Fe/H] > 0.30. One of these, HR 7373, is classified by Taylor as a SMR star. Castro et al. (1997) examined nine metal-rich dwarfs, with $m_{\rm v}$ as low as 11.3, and found that five have [Fe/H] > 0.30. Hence, while there are additional SMR stars than just those included Taylor's list, none of them are in the Bright Star Catalog, which is the source of Marcy and Butler's target list.

As an illustration of the unusual metallicity distribution of our program stars, we present in Fig. 5 the metallicity distribution of nearby G and K dwarfs from Favata et al. (1997) along with our spectroscopic [Fe/H] values; the peak of the distribution is -0.23. The mean metallicity of the parent stars of the nine planetary candidates is $+0.02$. Excluding HD 114762 and 70 Vir, which have the most massive companions, the mean metallicity of the remaining seven systems is $+0.11$. The mean metallicity of the four "51 Peg-like" systems is $+0.25$. This comparison is meant as a qualitative illustration only. To determine if our sample stars really have a higher mean metallicity than the nearby field stars, it will be necessary to compare their metallicities to the metallicity distribution of Marcy and Butler's target list. We have not yet done this, as the metallicity estimates of K and M dwarfs cannot yet be reliably determined to within 0.1 dex (for a discussion of problems associated with spectroscopic analyses of cool dwarfs, see Felzing & Gustafsson 1998).

The lithium abundances have been estimated recently for 51 Peg and 16 Cyg A and B. François et al. (1996) find that 51 Peg has a solar lithium abundance, less than our estimate. We do confirm the findings of Friel et al. (1993) and King et al. (1997) that the lithium abundances of 16 Cyg A and B differ greatly; King et al. derive $\log \epsilon({\rm Li}) = 1.27 \pm 0.05$ and < 0.6 for 16 Cyg A and B, respectively. The significance of these findings will be discussed in Sect. 4.5. A summary of published lithium estimates for the other stars in our program is given by King et al.

4.2. Ages, rotation periods, and masses

The $v \sin i$ estimates, when combined with the rotation periods and masses of the program stars, can be used to set limits on the masses of their companions. The rotation periods can be measured directly in those stars that exhibit variations in the Ca II H and K flux (Baliunas et al. 1996). Given that both age and angular velocity correlate fairly well with the mean Ca II flux for G dwarfs (Donahue 1993; Dorren et al. 1994; Soderblom 1985), the mean Ca II flux can also be used to estimate the rotation period. In this section we will estimate the ages, rotation velocities, and masses of the program stars and their companions.

The most reliable method of estimating the mass and age of an isolated field main sequence or subgiant star involves comparing its observed physical parameters ($T_{\rm eff}$, $M_{\rm V}$, [Fe/H]) to theoretical stellar evolutionary sequences. We make use of the Schaller et al. (1992) and Schaerer et al. (1993a,b) evolutionary stellar grids, to estimate their ages and masses. These theoretical tracks predict for the Sun a value of $T_{\rm eff}$ too high by 50 K and $M_{\rm V}$[5] too high by 0.08 mag. Therefore, in the following analysis we have added 50 K and 0.08 mag. to the measured $T_{\rm eff}$ and $M_{\rm V}$ values of the program stars when comparing them to the theoretical tracks.

We calculated $M_{\rm V}$ for each star using the *Hipparcos* parallaxes (ESA 1997); given the high precision of these parallaxes, the Lutz & Kelker (1973) correction was required only for HD 114762 (it is minor anyway). We list our age and mass estimates in Table 11. They were determined by visual inspection of the locations of the stars on the HR diagram relative to the isochrones with the appropriate metallicities. We employed the atmospheric parameters in Table 3 ($T_{\rm eff}$ and [Fe/H]) and the adopted $M_{\rm V}$ values (the listed values are the unaltered ones). We have also included υ And and τ Boo in the table, but with updated $M_{\rm V}$ values compared to those quoted in Paper I, which are based on pre-*Hipparcos* parallaxes.

Ng & Bertelli (1998) have derived updated ages for the stars in the Edvardsson et al. (1993) sample with more recent stellar evolutionary tracks and with $M_{\rm V}$ values based on *Hipparcos* parallaxes. They derived the ages and masses with a rigorous statistical methodology. We list in column 6 of Table 11 their age and mass estimates, which have typical uncertainties of 1 Gyr and 0.03 $\mathcal{M}_{\odot}$, respectively. The agreement between our estimates and those of Ng & Bertelli is quite good. Note, however, that they used the (incorrect) Edvardsson et al. (1993) value of [Fe/H] for 51 Peg; adopting [Fe/H] = 0.20 leads to a reduction in their age estimate for this star by 1.4 Gyr.

A consistency check on our Fe-line analysis of Sect. 3.1.1 is provided by the $\log g$ values derived from the evolutionary tracks (column 5 of Table 11). These $\log g$ estimates are very close our spectroscopic estimates, except for HD 114762, which is smaller. Of course, these two methods of estimating $\log g$ are not completely independent as both employ the same values of $T_{\rm eff}$.

There are two stars for which we could not obtain self-consistent solutions: τ Boo and ρ^1 Cnc. Our $T_{\rm eff}$ estimate for τ Boo is too hot by about 200 K for the ZAMS corresponding to its metallicity. Conversely, our $T_{\rm eff}$ estimate for ρ^1 Cnc is too cool by about 200 K. The discrepancy for τ Boo is not as serious, as our analysis of this star is less certain due to its broad lines. We do appear to have a problem with ρ^1 Cnc, though, which we will address further in Sect. 4.4.

There are other indicators that can be used to further constrain the ages of single stars. One of these relates to the mean level of chromospheric activity. Baliunas et al. (1998) quote ages derived from the mean level of Ca II activity, which we list in Table 11. The typical uncertainty in these age estimates is about 2 Gyr (Donahue 1998). Another age indicator relates

[5] We have adopted $M_{\rm V}$ = 4.82 for the Sun in all the analyses that require this quantity.

Table 11. Age and mass Estimates of the program stars derived from stellar evolutionary tracks

Star	$M_{\rm V}$	Age (Gyr)	Mass ($\mathcal{M}_{\odot}$)	$\log g$	Ng & Bertelli (1998) Age(Gyr), Mass($\mathcal{M}_{\odot}$)	Ca II Age (Gyr)
ρ^1 Cnc	5.47±0.03	$\gg$16	∼0.7	∼4.3		5
ρ CrB	4.18±0.03	11±2	0.96±0.03	4.18±0.05	12.1, 0.93	6
16 Cyg A	4.32±0.04	9±2	1.00±0.03	4.25±0.05		-
16 Cyg B	4.60±0.04	9±2	0.97±0.03	4.33±0.05		7
51 Peg	4.52±0.04	6±2	1.05±0.03	4.35±0.05	7.0, 1.10	10
47 UMa	4.29±0.03	8±2	1.03±0.03	4.27±0.05	6.5, 1.06	7
70 Vir	3.68±0.04	8.5±1.0	1.10±0.02	3.88±0.03		9
HD 114762	4.23±0.13	14±2	0.82±0.03	4.23±0.05	16, 0.78	5
υ And	3.45±0.03	2.5±1	1.31±0.04	4.20±0.04	2.7, 1.28	5
τ Boo	3.53±0.03	<1	∼1.36	∼4.27		2

The age, mass, and $\log g$ values were derived from the Schaller et al. (1992) and Schaerer et al. (1993a,b) stellar evolution grids using $M_{\rm V}$ and our $T_{\rm eff}$ and [Fe/H] estimates from Table 3. The Ca II age estimates are from Baliunas et al. (1998), except HD 114762, which is from Henry et al. (1997). These age estimates supercede those given by Gonzalez (1997; 1998), who employed older (and less accurate) stellar evolutionary grids in deriving these quantities. See text for additional details.

to the space motion in the Milky Way. As a star ages, chance encounters with molecular clouds perturb it away from a simple circular orbit in the plane of the disk. Therefore, the space velocity of a star generally increases with time. Of our sample, HD 114762 has the largest space velocity, as expected. Related to the level of chromospheric activity is the amplitude of the visual brightness variations; by the time a solar-type dwarf is about 3 Gyr old, the brightness variations drop below about 10 millimags (Dorren et al. 1994). High precision photometric monitoring of these stars by two groups (Guinan 1995; Henry et al. 1997) place upper limits of no more than a few millimags, indicating ages at least as great as the Sun's (even τ Boo appears constant at the millimag level even though it is young according to our analysis). Additional monitoring will be required to determine if long-term variations exist.

Rotation periods have been estimated for these stars from Ca II observations, either with a mean Ca II activity-rotation period relation, or more directly by detecting a periodic modulation of the Ca II flux. The rotation periods are given in Table 12. The only star on our program not listed by Baliunas et al. (1998) is HD 114762. Using the Ca II activity-rotation period relation of Noyes et al. (1984), Henry et al. (1997) derive a rotation period of 12±2 days for HD 114762. This estimate is clearly incompatible with its great age; we will adopt a value of 54 ± 12 days for this star (using Dorren et al.'s 1994 rotation-age relation). Also, 70 Vir is clearly evolved off the main sequence, so Noyes et al.'s relation will underestimate its rotation period. The value quoted by Baliunas et al. (1998), 36 days, has been increased by a factor of three, assuming simple conservation of angular momentum. A lower limit of 2 days was chosen for the uncertainties (except for τ Boo, which has a very short rotation period) due to the presence of surface differential rotation in solar type stars, which leads to a modulation of the apparent rotation period on timescales of a decade (Donahue 1993).

Using the adopted values of $\upsilon \sin i$, rotation period, and radius for each star, we calculated $\sin i$ for each star. The value for 16 Cyg B is from Hale (1994). The estimates for 16 Cyg B and 51 Peg are problematic; both are greater than 1.0. If the rotation period listed in Table 12 for 51 Peg is correct, then most of the published $\upsilon \sin i$ estimates for this star are too large; a value of 1.6 km s^{-1}, which is consistent with our estimate and that of Soderblom (1982), would give a value of $\sin i$ near 1.0. Obviously, values of $\sin i > 1.0$ are not acceptable. Taking this into account, we list the final $\sin i$ values in Table 12. One additional source of uncertainty needs to be included - the degree of misalignment between the orbital axis of the companion and rotational axis of the parent star, which we will represent as $\mid i_{\rm orb} - i_{\rm rot} \mid = \delta i$. Hale (1994) estimated that δi is about 10 degrees for solar-type binaries with semimajor axes less that 15 AU. Perhaps more relevant to the present analysis is the fact that the value of δi for Jupiter is only about 6 degrees. Including an additional uncertainty of 8 degrees in the orbital inclination, the final values of the orbital inclinations of the companions are listed in column 5 of Table 12. The companion masses were calculated from the mass function estimates given in the respective discovery papers (listed in the Introduction) and our estimates of the inclinations. They are given in the final column of Table 12.

Now that we have estimates of the masses of the planetary companions, their true nature can be constrained, assuming, of course, that the radial velocity variations are not intrinsic to the stars' photospheres. The results in Table 12 indicate that 70 Vir b and HD 114762 b are brown dwarfs or possibly even very low mass M dwarfs (for a contrary view, see Lin & Ida 1997 and Weidenschilling & Marzari 1996). The companions of τ Boo, ρ CrB, and 47 UMa are also quite massive and might be brown dwarfs. Those companions most securely in the giant planet mass regime are 16 Cyg B b, 51 Peg b, and υ And b (ρ^1 Cnc is an anomaly at this time).

Of relevance to 51 Peg is the fact that tidally locked close binaries (orbital periods of a few days) have lithium abundances larger than their single star counterparts (Soderblom et al. 1990; Balachandran et al. 1993). If, contrary to our findings, the 51 Peg

Table 12. Derived physical parameters of planetary systems

Star	Radius ($\mathcal{R}_\odot$)	Rotation Period (days)	$\sin i$	i (deg)	Planet Mass ($\mathcal{M}_{\rm J}$)
ρ^1 Cnc	0.98±0.07	42±2	< 1	< 90	> 0.66
ρ CrB	1.36±0.07	17±5	0.37 ± 0.17	22^{+19}_{-18}	$2.9^{+13.6}_{-1.3}$
16 Cyg B	1.14±0.06	(28)±2	$1.00^{+0.00}_{-0.17}$	90^{+0}_{-42}	$2.0^{+1.1}_{-0.3}$
51 Peg	1.15±0.05	37±2	$\simeq 1.0$	90^{+0}_{-8}	0.49 ± 0.03
47 UMa	1.26±0.05	(21)±2	0.69 ± 0.18	44^{+24}_{-21}	$3.4^{+3.1}_{-1.1}$
70 Vir	1.89±0.08	(108)±20	< 0.67	< 50	> 9.4
HD 114762	1.24±0.13	(54)±12	< 1	< 90	> 10.4
υ And	1.54±0.06	(12)±2	$1.00^{+0.00}_{-0.11}$	90^{+0}_{-35}	$0.76^{+0.19}_{-0.03}$
τ Boo	1.31±0.06	3.3±0.5	$0.72^{+0.18}_{-0.50}$	46^{+44}_{-41}	$5.9^{+43.9}_{-1.8}$

The rotation periods are from Baliunas et al. (1998), except for 70 Vir and HD 114762, which are derived in the text; those in parentheses are based on a mean Ca II activity-rotation period relation.

system has a very small orbital inclination and its companion is of stellar mass, then its lithium abundance would likely have been larger than we measured. This argument is less relevant to the other 51 Peg-like systems because: 1) υ And and τ Boo are young and hence expected to have larger lithium abundances, 2) ρ^1 Cnc's orbital period is longer, making tidal effects less important. Also, the rotation period of 51 Peg does not allow the possibility that this is a tidally locked system (Mayor & Queloz pointed out that the lack of synchronization on Gyr timescales is a strong argument against a stellar mass companion for 51 Peg).

4.3. Possible sources of high [Fe/H]

The high [Fe/H] values of 51 Peg and ρ^1 Cnc (also υ And and τ Boo) require explanation. It is too much to ascribe to coincidence the presence of two SMR stars and two stars very near the SMR limit in our small sample of planetary system candidates. In Paper I we suggested that the original photospheric compositions of the "51 Peg-like" systems had been altered by the same processes that lead to the creation of these unusual planetary systems.

Lin et al. (1996) have proposed that 51 Peg b, if it is indeed a gas giant, was formed at about 5 AU from the star and, at early times (within a few million years of its formation), migrated inward as a result of interactions with the circumstellar disk. The disk material (and presumably protoplanets) inside the orbit of 51 Peg b would likely have fallen into the star. Since much of it would have been inside the so-called "ice-boundary", much of the solid-state material would have consisted of refractory elements (essentially everything except H and He). This accreted material would have been mixed throughout the convective envelope of the parent star.

Using the Solar System as a model, we can estimate the effect on its photospheric abundances had the Sun ingested the equivalent of Mercury, Venus, Earth, and Mars in its early history. Sackmann et al. (1993) calculate that at an age of about 30 Myrs the convective region of the Sun contained about 0.03 $\mathcal{M}_\odot$. Assuming a composition similar to the C1 chondrites (Anders & Grevesse 1989), the addition of the terrestrial planets at this time would have dumped 2.18 x 10^{27} g of Fe into the convection zone, leading to an increase of [Fe/H] in the photosphere of 0.01 dex. The addition of 20 $\mathcal{M}_\oplus$, which is still only 0.06 $\mathcal{M}_{\rm Jup}$, would have resulted in an increase of 0.11 dex, a detectable change. The timing of the accretion is critical, as the stellar convection zone rapidly shrank in size during the first few million years of the Sun's existence - add the material too early, and it is diluted throughout a large volume; the timescale for the evolution of the protostellar disk is about 5 Myr (Strom et al. 1993).

What would have happened to the photospheric abundances of the early Sun if Jupiter were thrown into the convective envelope? The answer to this question depends on the bulk composition of Jupiter. If it is the same as the Sun's photosphere, then there will be no change in the Sun's metallicity. Estimates of the bulk composition of Jupiter indicate that it is enhanced in metals by about a factor of two relative to the Sun (Hubbard 1989); this is equivalent to about 10 $\mathcal{M}_\oplus$ of chondritic material mixed with 308 $M_\oplus$ of H and He. Given this, adding Jupiter would increase the Sun's photospheric metallicity by about 0.05 dex. Adding two Jupiters would increase it by 0.08 dex.

Alexander (1967) suggested that the injestion of a planet by a giant star can result in a large increase in its photospheric lithium abundance. Brown et al. (1989) resurrected this mechanism to try to account for the anomously high lithium abundances they measured in a few field giants. The present solar photospheric abundance of lithium is just over two dex less than the meteoritic abundance. This is commonly interpreted in terms of a gradual depletion of lithium in the envelope of the Sun on a billion year timescale. The addition of Jupiter to the present Sun would boost the lithium abundance by about 1.5 dex, while a very early ingestion would have boosted the lithium abundance by only 0.05 dex. The addition of the terrestrial planets to the present Sun would increase the lithium abundance by about 0.8 dex. Since lithium depletion in a solar-type star is probably not linear in time, the degree of its enhancement due to the addition of a planet depends sensitively on the timing of the injestion. Hence, the lithium abundances we have estimated for the par-

ent stars of the planetary candidates are not easy to interpret, given the uncertainty of the age estimates and given the as yet incompletely understood mechanisms of lithium depletion. It is interesting to note, however, that ρ CrB, 51 Peg, and 47 UMa, which appear to be older than the Sun, have significantly higher lithium abundances. Particularly valuable is the case of 16 Cyg A and B, which have significantly different lithium abundances (to be discussed in Sect. 4.5).

The next logical question to ask is, Why did the Solar System and the 51 Peg-like systems evolve differently? The metallicities of the parent stars appear to be the most significant differences. If 51 Peg was originally slightly more metal-rich than the Sun, then this would have resulted in the formation of a protoplanetary disk more abundant in refractory elements, which might have led to the more rapid formation of protoplanets. A slightly more massive disk also might have led to greater transfer of mass into the parent star (Laughlin & Bodenheimer 1994). Hence, according to this scenario, a more metal-rich star is more likely to alter its surface composition during the protostellar disk evolution phase than a similar but less metal-rich one. This is consistent with the similarity of the Solar System to the 47 UMa system, which has a solar metallicity parent star. The companion of 47 UMa orbits at about 2 AU in a low eccentricity orbit (Butler & Marcy 1996), apparently having avoided the orbital decay phenomenon proposed to have been experienced by 51 Peg's planet. However, ρ CrB is more metal-poor than 47 UMa, and its companion orbits closer to its parent star. Clearly, the diversity of the extrasolar systems shows that such a simple model is unlikely to fully account for the observed correlations between planets and the metallicities of their parent stars.

One additional piece of circumstantial evidence in favor of the self-enrichment scenario, noted in Paper I, is the scarcity of metal-rich giant stars. If the envelope of a 51 Peg-like system is metal-rich, then as it ascends the giant branch, the metallicity of its photosphere will decrease as the deepening convection zone is diluted with deeper more metal-poor layers. However, Taylor's (1996) claim that there are no definite SMR K giants needs to be revised; Castro et al. (1996) have performed a detailed abundance analysis of μ Leo finding that [Fe/H] = 0.46 $\pm$ 0.14. Hence, there are at least eight SMR dwarfs and one SMR giant in The Bright Star Catalogue.

If the photospheres of the parent stars of the 51 Peg-like systems are metal-rich relative to their interiors, then the evolutionary ages derived above are not correct. The metallicity affects not only the effective temperature and radius but also the luminosity. A reduced interior metallicity leads to a larger core mass and hence a greater luminosity (Jeffery et al. 1997).

Finally, we need to address the possibility that the high metallicities of the 51 Peg-like systems are primordial. Certainly, there is a spread in the metallicities (or oxygen abundances) of young stars and nebulae at the Sun's galactocentric distance (see Smartt & Rolleston 1997 for a summary of the observational evidence). The Sun itself is near the upper envelope of the metallicity distribution. One traditional explanation for this is that the Solar System formed in a metal-rich clump in the (inhomogeneous) ISM. In Paper I we suggested that the Sun might have been self-enriched during the planet formation process. However, the α Cen system, which is about the same age, is even more metal-rich than the Sun. Tripicco et al. (1995) derive an age and [Fe/H] value of the open cluster NGC 6791 of about 10 Gyr and [Fe/H] $\sim$ 0.3, respectively. Hence, clusters like NGC 6791, although very rare, might account for the existence of the 51 Peg-like stars.

4.4. ρ^1 Cnc

A number of our results concerning ρ^1 Cnc seem inconsistent. For instance, in Sect. 3.2 we derived a value of $\zeta_{\rm RT}$ from equation 1, which is much smaller than we measured directly on its spectrum and also smaller than the value predicted by Eq. 2; however, Eq. 2 gives a similar value to the measured value. Its $M_{\rm V}$ and $T_{\rm eff}$ parameters place it in the subgiant region of the HR diagram, implying an age much greater than the currently accepted range for the age of the universe. Cayrel de Strobel (1987), in her review of 30 SMR dwarfs and subgiants (at that time defined as being more metal-rich than the Hyades), also derived an extremely high age for ρ^1 Cnc (one other star in the sample, HD 190248, also appeared to have an extreme age). The low surface gravity we derived from our spectroscopic analysis ($\log g = 4.15$) appears to confirm its subgiant status; the surface gravity for G dwarfs ranges from about 4.4 to 4.5. Neuforge-Verheecke & Magain (1997) derived $\log g = 4.5$ for α Cen B, a metal-rich K1V dwarf. Baliunas et al. (1997) also note that their spectrum of ρ^1 Cnc is a better match to a subgiant than it is to a dwarf (see their paper for a discussion of previous studies bearing on this subject).

We have derived additional temperature estimates for ρ^1 Cnc from Johnson $B-V$ and $R-I$ photometry given by Gliese & Jahreiss (1991). The equations relating $T_{\rm eff}$, $\log g$, and [Fe/H] to $B-V$ and $R-I$ were derived from the synthetic colors given by Buser & Kurucz (1992). Corrections were then applied to the equations to give the correct value of $T_{\rm eff}$ for α Cen B (using the results of the spectroscopic analysis of Neuforge-Verheecke & Magain 1997) from its observed colors. The resulting values of $T_{\rm eff}$ for ρ^1 Cnc from its $B-V$ and $R-I$ colors are 5195 and 5460 K, respectively (this compares with $T_{\rm eff}$ = 5150$\pm$75 K from our spectroscopic analysis). The corresponding values for the K0IV star δ Eri are 4895 and 5035 K, respectively; Morell et al. (1992) derived $T_{\rm eff}$ = 4800 K for this star. The corresponding values for the G8V star HR 509 are 5385 and 5429 K, respectively; Morell et al. (1992) derived $T_{\rm eff}$ = 5300 K for this star. Note, if our spectroscopic $T_{\rm eff}$ estimate for ρ^1 Cnc is too low, then its true [Fe/H] value is even higher than than our estimate of 0.29, which is already unusually high. Arribas & Martinez Roger (1989) derived $T_{\rm eff}$ = 5100 $\pm$ 150 K and θ = 0.736 $\pm$ 0.043 mas for ρ^1 Cnc by applying the infrared flux method to its optical and infrared colors. This angular size corresponds to a physical size similar to that of the Sun, which is too large for a late G or early K dwarf.

The ρ^1 Cnc system is part of a common proper-motion pair with an M3.5 dwarf. This allows the possibility of comparing the metallicities of the two components. We have approached

the problem in the following way: an equation relating M_V, $B-V$, and [Fe/H] was derived from a small sample of M dwarfs that are members of nearby common proper motion pairs (the sample is from the listing of Poveda et al. 1994); the metallicity of each M dwarf was equated to that of its brighter F or G dwarf companion; the relation was applied to ρ^1 Cnc's companion in order to determine [Fe/H]. The result is [Fe/H] = -0.15 $\pm$ 0.31, where the uncertainty was calculated from the residuals of the calibrating stars. A similar equation was derived for G and K dwarfs and applied to ρ^1 Cnc. Our result is [Fe/H] = 0.32 ± 0.08, nearly identical to our spectroscopic estimate. This is only a preliminary analysis. A larger sample of M dwarfs will be required to reduce the uncertainty in this method to a level that may give us a definitive answer. This might best be accomplished with observations of a nearby solar-age open cluster with well-determined parameters.

Marcy & Butler (1998) have noted the presence of a long-term trend in the velocity residuals of ρ^1 Cnc after subtracting the main 14.6 day variation. They attribute the residuals to the presence of a companion with a minimum mass of 10 $\mathcal{M}_J$ and an orbital period of about 20 years. Assuming a total system mass of $\sim 1\ \mathcal{M}_\odot$, the mean apparent separation should be about 0.60 arcseconds. McAlister et al. (1993) reported on the absence of a visual companion to ρ^1 Cnc from a single speckle observation. They would have been able to detect a companion with a separation from the primary between 0.038 and 2 arcseconds and no more than 3 magnitudes difference in brightness. Hence, it is unlikely that this object is contaminating the optical colors of the primary. A search with an infrared imager may prove fruitful, though.

At this time, then, the observations are inadequate to determine the true nature of ρ^1 Cnc. Three possible explanations of the data are: 1) our spectroscopic analysis is in error more than we claim, 2) the ρ^1 Cnc system is actually a nearly pole-on stellar spectroscopic binary (as opposed to a star-planet binary), 3) ρ^1 Cnc really is a subgiant. While we believe the first case to be unlikely, verification of our results for this star would be welcomed. The second case could be tested by searching for variations in the line profile shapes. A system of two different stars viewed almost exactly pole-on will be seen as a very small amplitude single-lined spectroscopic binary with line profile variations that correlate with the mean wavelength shift of the lines, and a spectroscopic analysis will give the wrong answer for what is assumed to be a single star. The third possibility requires an explanation as to why ρ^1 Cnc prematurely evolved into a subgiant.

4.5. 16 Cyg A and B

The 16 Cyg system is particularly valuable as a test case of the self-enrichment scenario, because, presumably, both stars formed simultaneously from the same interstellar cloud. We confirm previous claims that both stars have the same metallicities to within about 0.1 dex and yet very different lithium abundances. Cochran et al. (1997) were not able to detect any significant modulation in the velocity data for 16 Cyg A, which they monitored over the same time interval as 16 Cyg B, implying, but not proving, that it does not have a companion. Another unusual feature of the system is the very high orbital eccentricity, 0.63, of 16 Cyg B b. They pointed out that among the substellar companions there exists a sharp boundary in a plot of orbital eccentricity versus M$\sin i$ at about 10 $\mathcal{M}_J$, where the less massive companions all have small eccentricities, except 16 Cyg B b.

The unusual characteristics of the 16 Cyg system led Mazeh et al. (1997) to propose that the orbit of 16 Cyg B b had been altered from an orginally more nearly circular configuration by the gravitational perturbations of 16 Cyg A. The current separation between the two stars is about 840 AU. Mazeh et al. (arbitrarily) set the semi-major axis of the stellar binary at 1100 AU, and ran simulations with eccentricities of 0.60 and 0.85 (also arbitrarily chosen). The closest separation for the $e = 0.85$ case is 165 AU. If, however, e is nearer to unity, then the two stars approach within a few AU of each other. At such a close range, assuming each star started with a gas giant with a semi-major axis $\sim$ 2 AU, planet-planet interactions are possible at some periastron passages and could result in severe perturbations of the planetary orbits. One planet could be ingested by its parent star as a result of a close planet-planet encounter, leaving the other in an eccentric orbit. In summary, in this scenario star-planet perturbations would gradually pump-up the eccentricity of each planet until they were able to get sufficiently close to each other for planet-planet perturbations to become significant. Unfortunately, as admitted by Mazeh et al., there are too many free parameters in the 16 Cyg system to definitively test any given dynamical scenario. Other possible perturbations not addressed by them are those due to nearby star encounters and the Milky Way gravitational tidal force.

Our scenario might be tested, instead, by comparing the compositions of 16 Cyg A and B. The addition of a 2 $\mathcal{M}_J$ gas giant to a solar type star several billion years after its formation will increase the surface lithium abundance by about 1.7 dex. Currently, the lithium abundance of 16 Cyg A is about 0.8 dex greater than that of 16 Cyg B. Hence, within the self-enrichment scenario, 16 Cyg A swallowed its planetary companion at some intermediate age. Also important is the prediction that the iron abundance would increase by only a small amount if a gas giant is ingested (about 0.08 dex for a 2 $\mathcal{M}_J$ gas giant). Averaging our [Fe/H] estimates of 16 Cyg A and B with those of Friel et al. (1993), we obtain [Fe/H] = 0.08 ± 0.04 and 0.04 ± 0.04 for A and B, respectively. Thus, A and B have the same metallicities to within the quoted uncertainties, but it is notable that both studies[6] obtain a slightly higher [Fe/H] value for A (the older studies listed by Cayrel de Strobel 1997 also obtain a higher [Fe/H] for 16 Cyg A).

Self-enrichment is not the only explanation consistent with the 16 Cyg A and B system. Cochran et al. (1997) propose a scenario whereby the different lithium abundances in 16 Cyg

[6] Friel et al. adopt a mean [Fe/H] value of 0.05 ± 0.06 for the 16 Cyg system, but their individual results are 0.06 and 0.02 for A and B, respectively.

A and B are the result of different initial rotation rates, which were, in turn, the result of different circumstellar environments early on. In this picture, 16 Cyg A would have lacked a massive proto-planetary disk, which would have provided rotational braking to the star. With rotational breaking, angular momentum is redistributed in a low mass star's interior, leading to enhanced lithium depletion at the base of the convection zone. One weakness with the Cochran et al. model is that it does not explain why 16 Cyg B was formed with a massive proto-planetary disk, while 16 Cyg A was not. Unfortunately, the rotation periods of 16 Cyg A and B are not known from direct measurement; Hale (1994) quotes rotation periods of 26.9 and 29.1 days for 16 Cyg A and B, respectively, based on the mean Ca II flux.

Is it possible that differences in the lithium abundances between 16 Cyg A and B can be due to different rates of lithium depletion on long timescales? For example, Deliyannis & Ryan (1997) present evidence that the lithium abundances in the atmospheres of the metal-poor common proper pair HD 134439 and HD 134440 differ by over 1 dex. These are cool dwarfs ($T_{\rm eff} \sim 4800$ K) and differ in temperature by only about 200 K. This large difference in the lithium abundances is interpreted by Deliyannis & Ryan as the result of a strong temperature dependence on lithium depletion, which is seen to occur in dwarfs with $T_{\rm eff} < 5500$ K. The large observed difference in the lithium abundances between α Cen A and B (King et al. 1997) also fits this trend. However, given that 16 Cyg A and B differ in temperature by no more than 50 K and that they are above the 5500 K limit, it is unlikely that significant gradual differential lithium depletion is occurring in this pair.

4.6. Testing planet formation models

The observed metallicity distribution of the parent stars of extrasolar planetary systems should eventually (when the number statistics are better) help to choose between the two most popular planet formation mechanisms: core instability-accretion (CIA; reviewed by Podolak et al. 1993) and gravitational instability (GI; Boss 1997). In the formation of a gas giant, the CIA model requires first the buildup of a 10-15 $\mathcal{M}_\oplus$ rocky core via planetesimal accretion before a protoplanetary nebula loses most of its H and He inventory. Once its core is sufficiently massive to accrete and retain H and He, a gas giant will grow in mass very quickly. Hence, in this model, the formation of a gas giant should have a strong dependence on the metallicity of the parent cloud from which it formed. The GI model has gas giants forming through the breaking-up of a disk into clumps through its self-gravity. This model is essentially the reverse of CIA in that core formation is not the trigger of planet formation but rather a by-product. The GI model should have a much weaker dependence on the metallicity of the parent cloud. Note, that the formation of terrestrial planets is strongly dependent on metallicity since they consistent almost entirely of metals.

While both models are still in an immature state with regard to specific predictions, it should be possible to make predictions about the metallicity dependence of giant planet formation (possibly also including correlations with planet mass). Particularly valuable would be an examination of parameter space near the Brown dwarf boundary ($\sim 5 - 15 \mathcal{M}_{\rm J}$). Current high-precision radial velocity searches are uncovering companions over a large mass range, $\sim 1 - 80 \mathcal{M}_{\rm J}$ (Mayor et al. 1998). It should be very illuminating to compare the metallicity distributions of the parent stars of the Jupiter-mass companions with those of the Brown dwarf companions. Mayor et al. suggest that the discontinuities observed in the companion mass-function histogram and the companion mass-eccentricity plot are evidence of different formation mechanisms for objects below $2 - 3 \mathcal{M}_{\rm J}$ and above 5 $\mathcal{M}_{\rm J}$.

5. Summary

We have performed spectroscopic abundance analyses of seven recently announced extrasolar planetary system candidates. The metallicities are less than solar for ρ CrB and HD 114762, approximately solar for 70 Vir and 47 UMa, and greater than solar for ρ^1 Cnc, 16 Cyg B, and 51 Peg (also υ And and τ Boo, from Paper I). We have also estimated the projected stellar rotational velocities and employed them, along with other data, to estimate the most likely masses of the substellar companions of these stars. The companions of 70 Vir and HD 114762 fall in the brown dwarf mass range. The companions of υ And, 16 Cyg B, and 51 Peg have the smallest masses and are the best extrasolar planet candidates at this time.

The most surprising, and potentially most important, findings in this study are the high metallicities of ρ^1 Cnc and 51 Peg (and υ And and τ Boo). These results are consistent with the planetary orbital migration model, whereby a gas giant migrates to within a few hundredths of an AU of the parent star, the material between the planet and the star presumably being accreted onto the latter. If this is confirmed by future observations, then Galactic chemical evolution models will have to be revised accordingly.

Our results for ρ^1 Cnc are anomalous. A straight-forward interpretation of the data implies an age greater than that of the universe. We tentatively interpret the ρ^1 Cnc system as a nearly pole-on spectroscopic binary. Careful line-profile analysis should be capable of testing this interpretation, and detailed analysis of its M dwarf companion will allow us to compare the metallicities of the pair.

To improve the mass estimates of the companions, future research should be directed at refining the $v \sin i$ estimates through the use of high-resolution high-S/N spectroscopy, especially for 16 Cyg A and B. Additional theoretical work needs to be done on the planet migration process, the role of metallicity in the planet formation process, and stellar models with metal-rich envelopes. Also, we encourage observers to direct their planetary search efforts at the known SMR dwarfs and subgiants. Finally, we also encourage spectroscopic abundance analyses to be done on new systems as they are announced.

Acknowledgements. The author would like to thank especially David L. Lambert and Eric Bakker for obtaining high resolution spectra of the program stars at his request and for helpful discussions. Additional helpful comments were provided by Suchitra Balachandran, Don

Brownlee, Jocelyn Tomkin, George Wallerstein, and the anonymous referee. Thanks also go to Chris Sneden for use of his abundance analysis code and Robert Kurucz for use of his model atmospheres. This research has made use of the Simbad database, operated at CDS, Strasbourg, France. The research has been supported in part by the National Science Foundation (Grant AST-9315124), the Robert A. Welch Foundation of Houston, Texas, and the Kennilworth Fund of the New York Community Trust.

References

Alexander J. B., 1967, Observatory 87, 238
Anders E., Grevesse N., 1989, Geochim. Cosmochim. Acta 53, 197
Arribas S., Martinez Roger C., 1989, A&A 215, 305
Balachandran S., Carney B. W., Fry A. M., Fullton L. K., Peterson R. C., 1993, ApJ 413, 368
Baliunas S. L., Sokoloff D., Soon W., 1996, ApJ 457, L99
Baliunas S. L., Henry G. W., Fekel F. C., Soon W. H., 1997, ApJ 474, L119
Baliunas S. L., Donahue R. A., Soon W. H., Henry G. W., 1998, Activity Cycles in Lower Main Sequence and Post Main Sequence Stars: The HK Project. In: R. A. Donahue and J. A. Bookbinder (eds.) Cool Stars, Stellar Systems, and the Sun, Tenth Cambridge Workshop, Astronomical Society of the Pacific. San Francisco, in press
Baranne A., Mayor M., Poncet J. T., 1979, Vistas Astr. 23, 279
Boesgaard A. M., Lavery R. J., 1986, ApJ 309, 762
Boss A. P., 1997, Science 276, 1836
Brown J. A., Sneden C., Lambert D. L., Dutchover E., 1989, ApJS 71, 293
Buser R., Kurucz R. L., 1992, A&A 264, 557
Butler R. P., Marcy G. W., 1996, ApJ 464, L153
Butler R. P., Marcy G. W., Williams E., Hauser H., Shirts P., 1997, ApJ 474, L115
Campbell B., Walker G. A. H., Yang S., 1988, ApJ 331, 902
Castro S., Rich R. M., McWilliam A., Ho L. C., et al., 1996, AJ 111, 2439
Castro S., Rich R. M., Grenon M., Barbuy B., McCarthy J. K., 1997, AJ 114, 376
Cayrel de Strobel G., 1987, JA&A 8, 141
Cayrel de Strobel G., Soubiran C., Friel E. D., Ralite N., Francois P., 1997, A&AS 124, 299
Cochran W. D., Hatzes A. P., 1994, Ap&SS, 212, 281
Cochran W. D., Hatzes A. P., Hancock T. J., 1991, ApJ 380, L35
Cochran W. D., Hatzes A. P., Butler R. P., Marcy G. W., 1997, ApJ, 483, 457
Cunha K., Smith V. V., Lambert D. L., 1995, ApJ 452, 634
Deliyannis C. P., Ryan S. G., 1997, ApJ 480, 43
Donahue R. A., 1993, Ph.D. thesis, New Mexico State University
Donahue R. A., 1998, Stellar Ages Using the Chromospheric Activity of Field Binary Stars. In: R. A. Donahue and J. A. Bookbinder (eds.) Cool Stars, Stellar Systems, and the Sun, Tenth Cambridge Workshop, Astronomical Society of the Pacific, San Francisco, in press
Dorren J. D., Guinan E. F., Dewarf L. E., 1994, The Decline of Solar Magnetic Activity with Age. In: Caillault J-P. (ed.) Cool Stars, Stellar Systems, and the Sun, Eighth Cambridge Workshop. Astronomical Society of the Pacific, San Francisco, p. 399
Edvardsson B., Anderson J., Gustafsson B., et al., 1993, A&A 275, 101
ESA, 1997, The *Hipparcos* and *Tycho* Catalogue, ESA SP-1200
Favata F., Micela G., Sciortino S., 1997, A&A 323, 809
Feltzing, S., Gustafsson, B. 1998, A&A, in press
François P., Spite M., Gillet D., Gonzalez J.-F., Spite F., 1996, A&A 310, L13
Friel E., Cayrel de Strobel G., Chmielewski Y., et al., 1993, A&A 274, 825
Fuhrmann K., Pfeiffer M. J., Bernkopf J., 1997, A&A 326, 1081
Gliese W., Jahreiss H. 1991, Nearby Stars, Preliminary 3rd Version, Astron. Rechen-Institute, Heidelberg
Gonzalez G., Lambert D. L., 1996, AJ 111, 424
Gonzalez G., 1997, MNRAS 285, 403 (Paper I)
Gonzalez G., 1998, The Stellar Metallicity - Planet Connection. In: Rebolo R., Martin E. L., Zapatero Osorio M. R. (eds.) Brown Dwarfs and Extrasolar Planets Workshop. Astronomical Society of the Pacific, San Francisco, p. 431
Guinan E., 1995, IAU Circ. 6261
Gray D. F., 1977, ApJ 218, 530
Gray D. F., 1984, ApJ 281, 719
Gray D. F., 1992, The Observation and Analysis of Stellar Photospheres, Cambridge Univ. Press, Cambridge
Hale A., 1994, AJ 107, 306
Hale A., 1995, PASP 107, 22
Hatzes A. P., Cochran W. D., Johns-Krull C. M., 1997, ApJ 478, 374
Henry G. W., Baliunas S. L., Donahue R. A., Soon W. H., Saar S. H., 1997, ApJ 474, L503
Hubbard W. B., 1989, Structure and Composition of Giant Planet Interiors. In: Atreya S. K., Pollack J. B., Mathews M. S. (eds.) Origin and Evolution of Planetary and Satellite Atmospheres. University of Arizona Press, Tucson, p. 539
Jeffery C. S., Bailey M. E., Chambers, J. E., 1997, Observatory 117, 224
King J. R., Deliyannis C. P., Hiltgen D. D., et al., 1997, AJ 113, 1871
Kurucz R. L., 1993, ATLAS9 Stellar Atmosphere Programs and 2km/s Grid CDROM Vol. 13, Smithsonian Astrophysical Observatory
Kurucz R. L., Furenlid I., Brault J., Testerman L., 1984, Solar Flux Atlas from 296 to 1300 nm, National Solar Observatory
Latham D. W., Mazeh T., Stefanik R. P., Mayor M., Burki G., 1989, Nat 339, 38
Laughlin G., Bodenheimer P., 1994, ApJ 436, 335
Lin D. N., Bodenheimer P., Richardson D. C., 1996, Nat 380, 606
Lin D. N., Ida S., 1997, ApJ 477, 781
Lutz T. E., Kelker D. H., 1973, PASP 85, 573
Marcy G. W., Butler R. P., 1996, ApJ 464, L147
Marcy G. W., Butler R. P., 1998, Extrasolar Planets Detected by the Doppler Technique. In: Rebolo R., Martin E. L., Zapatero Osorio M. R. (eds.) Brown Dwarfs and Extrasolar Planets Workshop. Astronomical Society of the Pacific, San Francisco, p. 128
Marcy G. W., Butler R. P., Williams E., et al., 1997, ApJ 481, 926
Mayor M., Queloz D., 1995, Nat 378, 355
Mayor M., Udry S., Queloz D., 1998, The Mass Function Below the Substellar Limit. In: Donahue B., Bookbinder J. (eds.) Cool Stars, Stellar Systems, and the Sun, Tenth Cambridge Workshop. Astronomical Society of the Pacific, San Francisco, in press
Mazeh T., Krymolowski Y., Rosenfeld G., 1997, ApJ 477, L103
McAlister H. A., Mason B. D., Hartkopf W. I., Shara M. M., 1993, AJ 106, 1639
McCarthy J. K., Sandiford B. A., Boyd D., Booth J., 1993, PASP 105, 881
Morell O., Källander D., Butcher H. R., 1992, A&A 259, 543
Neuforge-Verheecke C., Magain P., 1997, A&A 328, 261
Ng Y. K., Bertelli G., 1998, A&A 329, 943

Noyes R. W., Hartmann L., Baliunas S. L., Duncan D. K., Vaughan A. H., 1984, ApJ 279, 763
Noyes R. W., Jha S., Korzennik S. G., et al., 1997, ApJ 483, L111
Podolak M., Hubbard W. B., Pollack J. B., 1993, Gaseous Accretion and the Formation of Giant Planets. In: Levy E., Lunine J. (eds.) Protostars and Planets III. University of Arizona Press, Tucson, p. 1109
Poveda A., Herrera M. A., Allen C., Cordero G., Lavalley C., 1994, Rev Mex A&A 28, 43
Sackmann I. -J., Boothroyd A. I., Kraemer K. E., 1993, ApJ 418, 457
Schaerer D., Charbonnel C., Meynet G., Maeder A., Schaller G., 1993a, A&AS 102, 339
Schaerer D., Meynet G., Maeder A., Schaller G., 1993b, A&AS 98, 523
Schaller G., Schaerer D., Meynet G., Maeder A., 1992, A&AS 96, 269
Smartt S. J., Rolleston R. J., 1997, ApJ 481, L47
Sneden, C., 1973, Ph.D. thesis, University of Texas
Soderblom D. R., 1982, ApJ 263, 239
Soderblom D. R., 1985, AJ 90, 2103
Soderblom D. R., Oey M. S., Johnson D. R. H., Stone R. P. S., 1990, AJ 99, 595
Strom S. E., Edwards S., Skrutskie M. F., 1993, Evolutionary Timescales for Circumstellar Disks Associated with Intermediate- and Solar-Type Stars. In: Levy E., Lunine J. (eds.) Protostars and Planets III. University of Arizona Press, Tucson, p. 837
Takeda Y., 1995, PASJ 47, 337
Takeda Y., Kato K., Watanabe Y., Sadakane K., 1996, PASJ 48, 511
Taylor B. J., 1996, ApJS 102, 105
Tomkin J., Edvardsson B., Lambert D. L., Gustafsson B., 1997, A&A 327, 587
Tripicco M. J., Bell R. A., Dorman B., Hufnagel B., 1995, AJ 109, 1697
Tull R. G., MacQueen P. J., Sneden C., Lambert D. L., 1995, PASP 107, 251
Walker G. A. H., Walker A. R., Irwin A. W., et al., 1995, Icarus 116, 359
Weidenschilling S. J., Marzari F., 1996, Nat 384, 619